Clamp Subunit Dissociation Dictates Bacteriophage T4 DNA Polymerase Holoenzyme Disassembly†

Patrice Soumillion,‡,§ Daniel J. Sexton,‡ and Stephen J. Benkovic*

Department of Chemistry, The Pennsylvania State University, 152 Davey Laboratory, University Park, Pennsylvania 16802

Received October 13, 1997; Revised Manuscript Received December 11, 1997

ABSTRACT: Clamp proteins confer processivity to the DNA polymerase during DNA replication. These oligomeric proteins are loaded onto DNA by clamp loader protein complexes in an ATP-dependent manner. The mechanism by which the trimeric bacteriophage T4 clamp protein (the 45 protein) loads and dissociates from DNA was investigated as a function of its intersubunit protein−protein interactions. These interactions were continuously monitored using a fluorescence resonance energy transfer (FRET) based assay. A cysteine mutant of the 45 protein was constructed to facilitate site-specific incorporation of a fluorescent probe at the subunit interface. This site was chosen such that FRET was observed between the introduced fluorescent probe and a tryptophan residue located on the opposing subunit. By use of this fluorescently labeled 45 protein, it was possible to obtain an estimate of an apparent trimer dissociation constant from either a cooperative (0.08 ± 0.04 μM^2 at 25 °C) or a noncooperative (0.51 μM and 0.17 μM at 25 °C) model. Upon mixing the fluorescently labeled 45 protein with a 45 protein containing 4-fluorotryptophan, a nonfluorescent tryptophan analogue, subunit exchange between the two variants of the 45 protein was observed according to a reduction in intersubunit FRET. Subunit exchange rate constants measured in the presence or absence of the clamp loader (44/62 complex), the polymerase (43 protein), and/or a primer template DNA substrate demonstrate (a) that the 45 protein is not loaded onto DNA by subunit exchange and (b) that the disassembly dissociation of a stalled holoenzyme from DNA is dictated by 45 protein subunit dissociation.

DNA replication requires intricate coordination of a multitude of different proteins to facilitate leading- and lagging-strand DNA synthesis (*1*−*3*). Discontinuous lagging-strand synthesis, in particular, requires periodic recycling of the replication machinery from a completed Okazaki fragment to a new primer. Our laboratory has attempted to investigate this recycling process by independently examining avenues of DNA polymerase holoenzyme assembly and disassembly (*4*).

DNA polymerases are generally not processive on DNA unless incorporated into a holoenzyme complex with accessory proteins. The accessory protein directly responsible for the enhanced processivity is the sliding clamp protein. Clamp proteins from yeast (PCNA), *Escherichia coli* (β clamp) and bacteriophage T4 (gene 45 protein) have been identified and shown to exhibit a high degree of structural homology, though limited sequence homology (reviewed in refs *3*, *5*, and *6*). Though the quaternary structure of the identified clamp proteins varies between homodimers (e.g. β clamp) and homotrimers (e.g., PCNA and the 45 protein), they all share a common ring shape and a similar secondary structure arrangement (*7*, *8*; J. Kuriyan, personal communication). Their ring-shaped structure has led to the suggestion that they function as processivity factors by encircling the DNA, thereby tethering the polymerase onto DNA via a protein−DNA concatenate.

The bacteriophage T4 DNA replication system has been shown to be a useful model system for DNA replication because it is composed of similar replication components that are composed of fewer proteins than their counterparts in higher organisms (*9*, *10*). At the core of the T4 replication machinery is the DNA polymerase holoenzyme, which consists of the 43 protein (the DNA polymerase) and the 45 clamp protein (*11*, *12*). The 45 protein has been shown to track along DNA (*13*−*16*). In addition to enhancing DNA polymerase processivity, this DNA tracking ability appears to be involved in the transcriptional activation of late bacteriophage T4 genes (*17*−*19*). Relative to the analogous proteins of *E. coli* (β clamp) and yeast (PCNA), the 45 protein is unstable on DNA (*20*; Sexton and Benkovic, unpublished experiments). Recently, the interaction between the 45 protein and the 43 protein was targeted to the carboxyl-terminal sequence of the polymerase (*21*, *22*). This contact increases the resident time of the holoenzyme on DNA (*11*, *22*).

The 45 protein is loaded onto DNA by the ATP hydrolysis-dependent activity of the gene 44/62 protein complex, which functions as the clamp loader of the T4 system (for reviews, see refs *9* and *10*). Recently, the catalytic nature of this process has been studied (*11*, *23*) and the accompanying protein−protein interactions were monitored (*24*, *25*). However, the molecular mechanism by which the ring-shaped

† This research was supported by the National Institutes of Health through PHS Grant GM13306 (S.J.B.).

* To whom correspondence should be addressed.

‡ Authors contributed equally to this paper.

§ Present address: Laboratoire de Biochimie Physique et des Biopolymères, Université Catholique de Louvain, Bâtiment Lavoisier, 1/1B Place L. Pasteur, B-1348 Louvain-la-Neuve, Belgium.

S0006-2960(97)02526-9 CCC: $15.00 © 1998 American Chemical Society
Published on Web 01/30/1998

45 protein is loaded onto DNA by the 44/62 complex has not yet been determined. Based on the closed ring structure of the 45 protein (J. Kuriyan, personal communication), substantial structural changes must be associated with DNA loading. The nature of this conformational change and the mechanism whereby it is transduced from the ATP hydrolysis-dependent activity of the 44/62 complex are unknown.

In this paper, we have developed a novel fluorescence resonance energy transfer based assay system to monitor intersubunit protein−protein interactions within the T4 DNA polymerase clamp in order to comment on the mechanism of clamp loading and holoenzyme disassembly from DNA. This work also constitutes a new example of using unnatural amino acids in proteins to study protein−protein interactions and should be amenable to other systems.

EXPERIMENTAL PROCEDURES

Reagents and Enzymes. Bacteriophage T4 genomic DNA, 4-fluorotryptophan (4 FW),[1] and streptavidin were obtained from Sigma, whereas IAEDANS was from Molecular Probes, and the casamino acids were from Difco. The restriction enzymes, the T4 DNA ligase, and the Deep Vent polymerase were all from New England Biolabs, Promega, or Boehringer Mannheim, and the dNTPs were obtained from Pharmacia. The T4 exonuclease-deficient polymerase D219A mutant was purified as described (*26*). The D219A mutant of the T4 polymerase was used in these studies to avoid complications arising from the presence of the exonuclease activity. The polymerase activity of the T4 D219A polymerase is identical with that of the wild-type enzyme (*26*). The 44/62 complex was purified to homogeneity as described elsewhere (*27*, *28*). The biotinylated forked DNA substrate, Bio34/62/36, was constructed and quantitated as described (*12*).

Strains and Plasmids. The *Escherichia coli* strains used were DH5α (Novagen), BL21(DE3) (Novagen), W3110 *trp*A33 (gift of Carl Frieden, Washington University), and W3110(DE3). W3110(DE3) was constructed by integrating the lDE3 prophage into the W3110 chromosome with the lysogenization kit from Novagen according to the instructions provided by the manufacturer. The lysogenized host was then used to express target genes cloned into pET vectors under control of the T7 promoter. The plasmids pET45C1 and pET45C6 contain the Thr7Cys and Val162Cys mutants of the 45 protein, respectively, cloned between the *Nde*I and *Bam*HI sites of pET-26b(+) expression vector (Novagen). The pET45C1 plasmid was a gift of John Kuriyan, Rockefeller University. The construction of pET45C6 is described below.

Mutagenesis. All primers were synthesized on a Perceptive Biosystems 8909 DNA synthesizer and deprotected according to the instructions provided by the manufacturer. Val162 was mutated to Cys using a PCR overlap extension procedure. The PCR reaction mixtures (100 μL) contained either 40 ng of T4 genomic DNA (primary PCRs) or 200 ng of each DNA fragment (secondary overlap PCR), 0.3 mM each dNTP, 0.5 μM each primer, and 1 unit of Deep Vent polymerase. The following PCR program was used: (i) 1 cycle with 5 min at 95 °C, 2 min at 50 °C, and 3 min at 72 °C; (ii) 3 cycles with 2 min at 95 °C, 1 min at 50 °C, and 3 min at 72 °C; (iii) 30 cycles with 2 min at 95 °C, 1 min at 57 °C, and 90 s at 72 °C; and (iv) 20 min at 72 °C. PCR was performed using a Perkin-Elmer thermocycler. A 512 bp fragment containing the V162C mutation was amplified with the following primers: 5′GCGGAATTCCATATGAAACTGTCTAAAGAT (forward primer) and 5′GAGTCAAAGAGTATTTACAACGGGTCAGAGC (mutagenic primer). Besides the V162C mutation, the mutagenic primer also introduced a silent mutation to suppress a *Ssp*I site present in the wild-type gene. The overlapping 546 bp fragment was amplified with the following primers: 5′GCGGAATTCGGATCCCTATTAAAAATCGTGGGT (reverse primer) and 5′GCAATTTACGATTTGAACGGTTTTCTCGG (inside primer). The two fragments were purified from a 1% SeaKem agarose gel using the Ultrafree-MC centrifugal filter device from Millipore (protocol from the manufacturer) and used in the overlap extension PCR with the forward and reverse primers. The final fragment (717 bp) was gel-purified in the same way, restricted with *Nde*I and *Bam*HI, and ligated into pET-26b(+) restricted with the same enzymes. After transformation into DH5α cells, the expected plasmid, pET45C6, was found by restriction with *Ssp*I and verified by DNA sequencing.

Preparation of Fluorescently Labeled V162C-45 Protein. The V162C-45 protein was expressed in BL21(DE3) cells containing the pET45C6 vector and purified to homogeneity as described for the wild-type (*28*) and stored in 20 mM Tris, 1 mM β-mercaptoethanol, 50 mM NaCl, 1 mM EDTA, and 10% glycerol, pH 7.5, at −70 °C. To label the cysteine thiol of V162C-45 protein, 1 mL of the above stock solution was diluted to 5 mL with 50 mM HEPES, 50 mM potassium acetate, 1 mM EDTA, and 10% glycerol, pH 7.8, containing 1 mM IAEDANS. The reaction was allowed to proceed at 4 °C in the dark for 16 h before dialysis against 3 × 1.5 L of 20 mM Tris, 1 mM β-mercaptoethanol, 5 mM EDTA, 50 mM NaCl, and 10% glycerol, pH 7.5, and subsequent storage at −70 °C. The final protein concentration was determined using a Bio-Rad (Bradford) protein assay where the wild-type 45 protein served as the protein standard. Using the IAEDANS molar extinction coefficient (5700 M^{-1} cm^{-1} at 340 nm) the labeling efficiency was found to be approximately 3 mol of AEDANS/mole of 45 protein trimer.

Incorporation of 4-fluorotryptophan into the 45 protein. 4-Fluorotryptophan (4FW) was incorporated into the 45 protein using a tryptophan auxotrophic *E. coli* strain containing the λDE3 prophage integrated into its genome. The obtained lysogenized host, W3110(DE3), contains the T7 RNA polymerase gene for use with pET expression vectors. W3110-DE3 cells were transformed with the pET45C1 plasmid and grown in a medium similar to that previously described (*29*, *30*). The medium is composed of casamino acids (12 g/L), $Na_2HPO_4 \cdot 7H_2O$ (12 g/L), KH_2PO_4 (3 g/L), NH_4Cl (1 g/L), NaCl (0.5 g/L), all the pyrimidine and purine bases (1 mM each), folate (1 mM), nicotinic acid (150 mM), thiamin (150 mM), riboflavin (150 mM), glucose (2 g/L), $FeCl_3$ (500 mg/L), $ZnSO_4$ (40 mg/L), $CuSO_4$ (80 mg/L), $CoCl_2$ (70 mg/L), $MnSO_4$ (50 mg/L), Na_2MoO_4 (70 mg/L),

[1] Abbreviations: 4FW, 4-fluorotryptophan; IAEDANS, 5-[[2-[(iodoacetyl)amino]ethyl]amino]naphthalene-1-sulfonic acid; HEPES, 4-(2-hydroxyethyl)-1-piperazineethanesulfonic acid; bp, base pairs; tris, tris(hydroxymethyl)aminomethane; EDTA, ethylenediaminetetraacetic acid; IPTG, isopropyl β-D-thiogalactopyranoside; dNTP, deoxynucleoside triphosphate; ATP-γ-S, adenosine 5′-*O*-(3-thiophosphate); BSA, bovine serum albumin; FRET, fluorescence resonance energy transfer.

$MgSO_4$ (1 mM), $CaCl_2$ (0.1 mM), kanamycin (25 mg/L), and L-tryptophan (2 mg/L). A 20 mL overnight culture in LB medium (*31*) containing kanamycin (25 mg/L) grown at 37 °C was centrifuged and resuspended in 1 L of sterile filtered medium. Cells were grown with shaking at 37 °C until they reached a stationary phase due to tryptophan starvation ($OD_{600\ nm} \sim 1.0$). At this point, IPTG and 4FW were added to final concentrations of 0.2 mM and 60 mg/L, respectively, to induce protein expression with 4FW incorporation. Cells were then incubated at 37 °C with shaking for an additional 3 h. The cells were harvested by centrifugation and the 4FW-45 protein was purified to homogeneity as described for the wild type (*28*). The final protein concentration (80 μM) was determined by using an extinction coefficient corrected for the 4FW substitutions (*32*): 46 900 M^{-1} cm^{-1} at 265 nm rather than 57 200 M^{-1} cm^{-1} at 280 nm for the wild-type protein (*10*). Protein aliquots were stored at −70 °C.

ATPase Activity Assay. Variants of the 45 protein were assayed for proper functionality according to their ability to substitute for the wild-type 45 protein in stimulating the 44/62 complex ATPase activity. ATPase assays were performed spectrophotometrically as previously described using an enzyme-coupled system in complex buffer (25 mM Tris, 150 mM potassium acetate, 10 mM magnesium acetate, and 10 mM β-mercaptoethanol, pH 7.5) (*23*).

Steady-state fluorescence spectroscopy. Steady-state fluorescence spectroscopy was performed using either a SLM Aminco 8000C or a Photon Technology International spectrofluorometer (model QM1) equipped with a thermostated cell compartment that was maintained at 25 °C. Excitation and emission slit widths were each maintained at 4 nm. All fluorescence spectra were corrected for background fluorescence.

Stopped-Flow Fluorescence Spectroscopy. Stopped-flow fluorescence measurements were performed using an Applied Photophysics stopped-flow instrument at a constant temperature of 25 °C. The excitation wavelength was fixed at 290 nm and a cutoff filter was placed in the detector to follow fluorescence emission above 420 nm.

Model of 45 Protein Subunit Dissociation. The fluorescence dilution data (Figure 2) were fit according to the following oligomerization model (45 monomer = A):

$$[A_3] \overset{K_{d1}}{\rightleftharpoons} [A] + [A_2]$$

$$[A_2] \overset{K_{d2}}{\rightleftharpoons} 2[A]$$

and

$$K_{d1} = [A][A_2]/[A_3] \quad (1)$$

$$K_{d2} = [A]^2/[A_2] \quad (2)$$

The 45 monomer concentration [A] can be expressed as a function of K_{d1}, K_{d2}, and the total 45 protein concentration ($[A_3]_0$):

$$[A]^3 + (2K_{d2}[A]^2/3) + (K_{d1}K_{d2}[A]/3) - K_{d1}K_{d2}[A_3]_0 = 0 \quad (3)$$

This cubic equation was solved for [A] either using the Mathematica computer program or according to Weast and Selby (*33*) and the data were fit to the following equations for noncooperative (eq 4) and cooperative (eq 5) dissociation:

$$F = F_A[A]/[A_3]_0 + F_{A2}[A_2]/[A_3]_0 + F_{A3}[A_3]/[A_3]_0 \quad (4)$$

where F is the observed specific fluorescence (fluorescence/$[45_t]_0$), F_A is the specific fluorescence of the monomeric 45 protein, F_{A2} is the specific fluorescence of the dimeric 45 protein, and F_{A3} is the specific fluorescence of the trimeric 45 protein.

$$F = F_A[A]/[A_3]_0 + F_{A3}[A_3]/[A_3]_0 \quad (5)$$

Scheme 1: Subunit Exchange Simulation Mechanism

$A_2 + A \underset{k_{-1}}{\overset{k_1}{\rightleftharpoons}} A_3$

$B_2 + B \underset{k_{-1}}{\overset{k_1}{\rightleftharpoons}} B_3$

$AB + A \underset{k_{-2}}{\overset{k_2}{\rightleftharpoons}} A_2B$

$A_2 + B \underset{k_{-3}}{\overset{k_3}{\rightleftharpoons}} A_2B$

$AB + B \underset{k_{-2}}{\overset{k_2}{\rightleftharpoons}} AB_2$

$A + B_2 \underset{k_{-3}}{\overset{k_3}{\rightleftharpoons}} AB_2$

$A + A \underset{k_{-4}}{\overset{k_4}{\rightleftharpoons}} A_2$

$B + B \underset{k_{-4}}{\overset{k_4}{\rightleftharpoons}} B_2$

$A + B \underset{k_{-5}}{\overset{k_5}{\rightleftharpoons}} AB$

Simulation of 45 Protein Subunit Exchange. The subunit exchange kinetic data were simulated using the PC version of the KinSim program (*34*) with a mechanism that allowed dissociation of the trimeric 45 protein to occur through dimers to monomers and then recombine with the nonfluorescent subunits (Scheme 1 and Discussion).

RESULTS

Construction of the V162C-AEDANS-45 Protein. On the basis of the recently determined crystal structure of the 45 protein (J. Kuriyan, personal communication), we constructed a variant of the 45 protein to permit observation of intersubunit fluorescence resonance energy transfer (FRET) between an interfacial tryptophan residue and a fluorescent probe conjugated to a genetically introduced cysteine residue on the opposing subunit. Since the wild-type 45 protein does

Table 1: Stimulation of the 44/62 Complex Steady-State ATPase Activity by Variants of the 45 Protein[a]

45 protein	ATPase rate 1[b] (nM/s)	ATPase rate 2[b] (nM/s)
WT 45	325 ± 5.9	43 ± 6
4FW-45	332 ± 12	17 ± 2
V162C	356 ± 22	45 ± 7
V162C-45-AEDANS	124 ± 10	18 ± 1

[a] Activity measurements were performed as described (*23*) in the presence of 250 nM proteins, 1 mM ATP, 250 nM Bio34/62/36mer DNA, 3 mM PEP, 0.2 mM NADH, and 3 units/mL each of lactate dehydrogenase and pyruvate kinase in complex buffer (25 mM Tris, 150 mM potassium acetate, 10 mM magnesium acetate, and 10 mM β-mercaptoethanol, pH 7.5). [b] ATPase rate 1 refers to the ATPase activity of the 44/62 complex observed in the presence of the 45 protein and DNA. ATPase rate 2 refers to the diminished ATPase rate observed upon addition of the T4 DNA polymerase (the 43 protein) to the above mixture.

not contain any cysteine residues, the introduction of a cysteine residue by site-directed mutagenesis facilitates site-selective thiol modification with a fluorescent probe. Valine 162 was chosen for replacement by a cysteine residue on the basis of its position at a solvent-accessible site within the subunit interface in close proximity to one of the two tryptophan residues present in each subunit. The V162 position is separated by less than 15 Å from W91, the closest tryptophan of the opposing subunit, and greater than 25 Å from W198, the only other tryptophan within the subunit. Therefore, thiol modification of the V162C-45 protein with an acceptor of tryptophan fluorescence, such as IAEDANS, should allow observation of intersubunit FRET.

Construction of 4FW-45 Protein. 4-Fluorotryptophan (4FW) is a nonfluorescent tryptophan analogue that can be biosynthetically incorporated into proteins (*32*). The incorporation of 4FW into the 45 protein was achieved by inducing protein expression in an *E. coli* tryptophan auxotroph in the presence of excess 4FW. The high efficiency of protein expression usually observed with pET vectors was maintained using 4FW in place of tryptophan in the expression medium since approximately 50 mg of pure 4FW-45 was obtained from a 1 L culture. The omission of 4FW during IPTG induction resulted in an undetectable amount of 45 protein according to SDS−PAGE and Coomassie stain analysis (data not shown). The plasmid (pET45C1) used to incorporate 4FW encodes a T7C mutant of the 45 protein. The T7C-45 protein has been previously demonstrated to behave as wild-type (*24*).

Activity of the Modified 45 Proteins. The degree to which the ATPase activity of the 44/62 complex is stimulated by the variants of the 45 protein provides a convenient assay to assess the effects of derivatization on 45 protein function (Table 1). ATP is consumed as the 44/62 protein pair loads the 45 protein onto the Bio34/62/36 DNA substrate. As the 45 protein dissociates from DNA, it is reloaded by 44/62 with additional ATP hydrolysis. It is this dissociation event that has been implicated to limit the observed steady-state ATPase k_{cat} (*23*). The consumption of ATP is linked through an enzyme-coupled system to NADH depletion, which is monitored according to a decrease in the absorbance at 340 nm (*23*). The addition of the T4 DNA polymerase diminishes ATP consumption through the formation of holoenzyme, which is more stable on DNA than the 45 protein alone (*11, 23*).

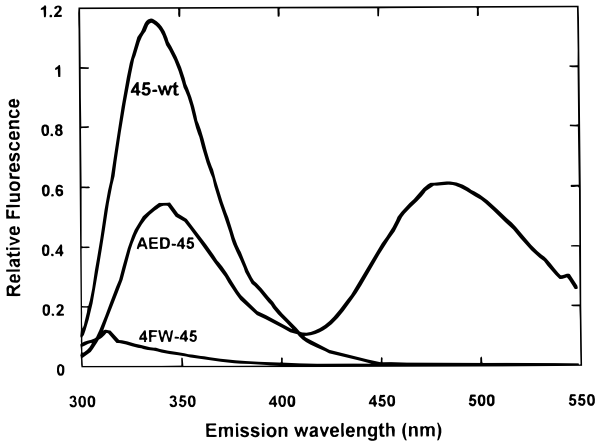

FIGURE 1: Fluorescence emission spectra of the variants of the 45 protein. Each emission spectrum was obtained using an excitation wavelength of 280 nm where 45-wt is the wild-type 45 protein, AED-45 is the V162C-AEDANS-45 protein, and 4FW-45 is the 45 protein containing 4-fluorotryptophan. All protein concentrations were 200 nM in complex buffer as defined in Experimental Procedures.

As shown in Table 1, the 4FW-45 protein and the V162C-45 protein stimulated the ATPase activity of the 44/62 complex to approximately the same extent as the wild-type 45 protein, both before and after the addition of the polymerase. When the V162C thiol was alkylated with IAEDANS, the resulting V162C-AEDANS-45 protein was still loaded onto DNA by the 44/62 complex, albeit with a slower steady-state rate of ATP hydrolysis. Upon addition of the T4 polymerase, the ATPase rate observed with the V162C-AEDANS-45 protein was shut down in a manner similar to that observed using the wild-type protein (Table 1).

Steady-State Fluorescence of the V162C-AEDANS-45 Protein. Excitation (λ_{ex} = 280 nm) of the V162C-AEDANS-45 protein produced a fluorescence emission spectrum with two fluorescence maxima (Figure 1). The first peak (λ_{max} at 340 nm) is primarily a consequence of the tryptophan fluorescence of the V162C-AEDANS-45 protein. Compared to the wild-type 45 protein, the specific tryptophan fluorescence (fluorescence/protein concentration) of the V162C-AEDANS-45 protein was found to be quenched by approximately 50% (Figure 1). The second peak (λ_{max} at 488 nm) is a consequence of fluorescence resonance energy transfer to the covalently attached fluorescent probe (AEDANS). The overlap of the excitation wavelength of the probe (λ_{ex} = 340 nm) with the emission wavelength of tryptophan enables energy transfer from the excited tryptophans to the fluorescent probe (*35*).

Steady-State Fluorescence of the 4FW-45 Protein. The residual fluorescence of the 4FW-45 protein, relative to the wild-type and the V162C-AEDANS-45 protein, is shown in Figure 1. The specific tryptophan fluorescence of the 4FW-45 protein was found to be decreased to approximately 5% that of the wild-type protein. This background fluorescence level is likely due to tyrosine fluorescence and/or to the adventitious incorporation of native tryptophan residues. The yield of 4FW incorporation in the 4FW-45 protein preparation was therefore estimated to be at least 95%.

Oligomerization of the 45 Protein. As expected, the intersubunit FRET signal is dependent upon the oligomerization of the 45 protein. Hence, the specific fluorescence

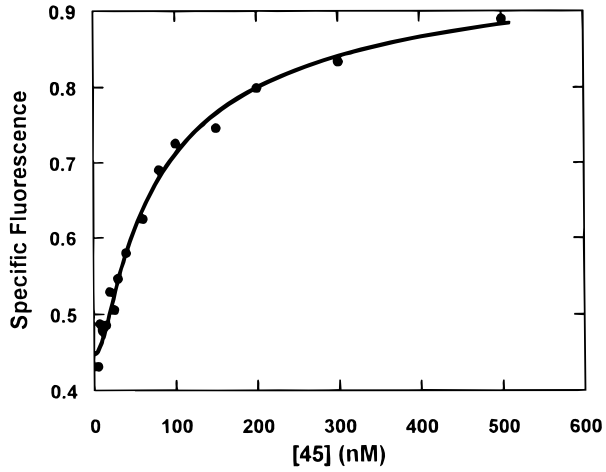

FIGURE 2: Oligomerization of the 45 protein at 25 °C. Fluorescence was monitored using a 290 nm excitation wavelength and a 488 nm emission wavelength at different concentrations of the 45 protein. The concentration of the V162C-AEDANS-45 protein was varied from 1 to 500 nM in complex buffer with 100 nM BSA included as a carrier protein. Each concentration was equilibrated at the required temperature for approximately 1 h prior to the fluorescence observation. The solid line represents the fit to eq 5.

Table 2: Fit Parameters to a Cooperative versus a Noncooperative Model of 45 Protein Oligomerization[a]

	25 °C		37 °C	
parameter	$K_{d1} \ll K_{d2}$[b]	$K_{d1} = 3K_{d2}$[b]	$K_{d1} \ll K_{d2}$	$K_{d1} = 3K_{d2}$
K_{d1}[c] (μM)	na[d]	0.51 ± 0.25	na	1.0 ± 0.5
K_{d2}[c] (μM)	na	0.17 ± 0.08	na	0.33 ± 0.17
$K_{d1}K_{d2}$ (μM^2)	0.08 ± 0.04	na	0.14 ± 0.04	na
F_A[e]	1.76 ± 0.10	1.35 ± 0.15	1.24 ± 0.10	0.97 ± 0.12
F_{A2}[e]	na	6.32 ± 0.35	na	5.73 ± 0.29
F_{A3}[e]	11.8 ± 0.3	14.9 ± 0.6	10.2 ± 0.3	14.2 ± 0.5
χ^2	0.73	1.6	1.5	3.9

[a] The fluorescence dilution data (Figure 2) were fit to eq 5 under cooperative or noncooperative conditions. [b] $K_{d1} \ll K_{d2}$ represents the cooperative model, whereas $K_{d1} = 3K_{d2}$ represents the noncooperative model. [c] K_{d1}, trimer to dimer dissociation constant; K_{d2}, dimer to monomer dissociation constant. [d] na, not applicable. [e] $F_{A,}$ specific fluorescence of the monomer; $F_{A2,}$ specific fluorescence of the dimer; $F_{A3,}$ specific fluorescence of the trimer. In the noncooperative model, F_{A2} is fixed equal to $F_A + F_{A3}/3$ in order to reduce the number of parameters to optimize. This assumption is derived from the fact that the dimer contains one subunit capable of inter-FRET signal and one subunit capable of only intra-FRET signal.

($\lambda_{ex} = 290$ nm; $\lambda_{em} = 488$ nm) of the V162C-AEDANS-45 protein at 25 °C was found to decrease as the protein concentration was lowered, signifying dissociation into dimers and/or monomers (Figure 2). A similar behavior was observed at 37 °C (data not shown). The data were fit to eqs 4 and 5 to provide an estimate of the apparent K_d from either a cooperative ($K_{d1} \ll K_{d2}$) or a noncooperative ($K_{d1} = 3K_{d2}$) model (Table 2, Figure 2). Table 2 compares the parameters from a fit to either a cooperative or a noncooperative model. It is evident that the cooperative model possesses lower χ^2 numbers than the noncooperative model.

Kinetic Analysis of 45 Protein Subunit Exchange. Upon mixing of the V162C-AEDANS-45 protein with the nonfluorescent 4FW-45 protein, spectral changes were observed in both the probe and tryptophan fluorescence. The observed fluorescence changes were consistent with a subunit exchange event between the V162C-AEDANS-45 protein and

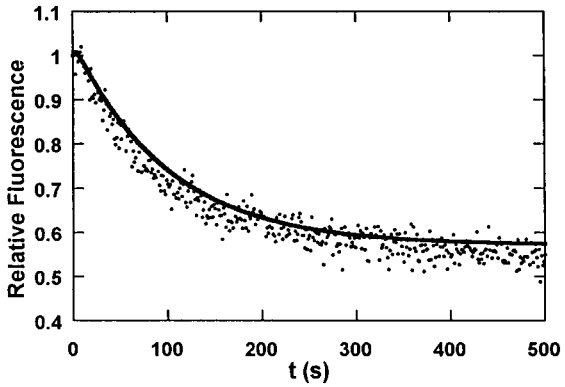

FIGURE 3: 45 Protein subunit exchange. The V162C-AEDANS-45 protein was mixed in a stopped-flow apparatus against the 4FW-45 protein so that the final protein concentrations were 0.5 μM and 2 μM, respectively, in complex buffer at 25 °C. The fluorescence emission resulting from excitation with 290 nm light was monitored above 420 nm using a cutoff filter. The data were fit (not shown) to a single-exponential function with an offset to yield the parameters included in Table 2, row 1. The data were also simulated (solid line) using the mechanism shown in Scheme 1 and the following rate constants, which are derived from the cooperative model (Table 2): $k_{-1} = 0.01$ s^{-1}; $k_1 = 10$ μM^{-1} s^{-1}; $k_{-2} = 0.0067$ s^{-1}; $k_2 = 10$ μM^{-1} s^{-1}; $k_{-3} = 0.0033$ s^{-1}; $k_3 = 10$ μM^{-1} s^{-1}; $k_{-4} = 1600$ s^{-1}; $k_4 = 20$ μM^{-1} s^{-1}; $k_{-5} = 1600$ s^{-1}; $k_5 = 40$ μM^{-1} s^{-1}. The initial protein concentrations for the simulation were calculated using the cooperative K_d value at 25 °C: $[A_3]_{(t=0)} = 151.5$ nM; $[A]_{(t=0)} = 144.5$ nM; $[B_3]_{(t=0)} = 1886$ nM; $[B]_{(t=0)} = 335.5$ nM. Conversion of the simulated concentration output to fluorescence was performed with the specific fluorescences reported in Table 4 and subsequent normalization. For comparison, the following rate constants were derived from the noncooperative simulation (not shown): $k_{-1} = 0.0193$ s^{-1}; $k_1 = 3.78$ μM^{-1} s^{-1}; $k_{-2} = 0.00643$ s^{-1}; $k_2 = 3.78$ μM^{-1} s^{-1}; $k_{-3} = 0.00129$ s^{-1}; $k_3 = 3.78$ μM^{-1} s^{-1}; $k_{-4} = 0.00643$ s^{-1}; $k_4 = 3.78$ μM^{-1} s^{-1}; $k_{-5} = 0.00643$ s^{-1}; $k_5 = 7.57$ μM^{-1} s^{-1}.

the 4FW-45 protein. As expected from such an event, the tryptophan fluorescence increased (data not shown) while the probe fluorescence diminished over time (Figure 3). Due to the nonfluorescent nature of the 4FW residue, the formation of the mixed protein species blocks intersubunit FRET. Direct excitation of the probe ($\lambda_{ex} = 340$ nm) during the subunit exchange experiment resulted in no significant fluorescence change, which suggests that the probe resides in a similar environment in the mixed subunit species (data not shown).

The decrease in probe fluorescence that occurred upon mixing 2 μM 4FW-45 protein with 0.2 μM V162C-AEDANS-45 protein was well approximated by a single-exponential function to yield a rate constant of $(9.9 \pm 0.4) \times 10^{-3}$ s^{-1} (Figure 3, Table 3). Monitoring the accompanying increase in tryptophan fluorescence provided an essentially identical rate constant (data not shown). This subunit exchange rate constant was found to be independent of protein concentration over an 8-fold range in protein concentrations (from 4 μM 4FW-45/1 μM V162C-AEDANS-45 protein to 500 nM 4FW-45/125 nM V162C-AEDANS-45 protein) (data not shown).

Effect of Complexation on 45 Protein Subunit Exchange. In the presence of either ATP or ATP-γ-S, a nonhydrolyzable ATP analogue, it was previously shown that a 45·44/62 complex is formed (*24*, *25*). The 45 protein subunit exchange rate constant measured while complexed to the 44/62 protein pair was slightly decreased (Table 3, rows 1−3).

Table 3: 45 Protein Subunit Exchange Rate Constants

solution A[a]	solution B[a]	$k_{exchange}$[b] (10^{-3} s^{-1})
(1) 0.2 μM AED-45[c]	2 μM 4FW-45	9.9 ± 0.9
(2) 0.2 μM AED-45, 2.2 μM 44/62, and 10 mM ATP	2 μM 4FW-45	6.7 ± 0.7
(3) 0.2 μM AED-45, 2.2 μM 44/62, and 1 mM ATP-γ-S	2 μM 4FW-45	7.1 ± 0.7
(4) 0.2 μM AED-45, 0.2 μM 44/62, 0.2 μM Bio34/62/36, and 10 mM ATP	2 μM 4FW-45	8.4 ± 0.7
(5) 0.2 μM AED-45, 0.2 μM 44/62, 0.2 μM Bio34/62/36, 0.2 μM 43, and 10 mM ATP	2 μM 4FW-45	3.3 ± 0.6

[a] Indicated concentrations are final concentrations obtained upon mixing the two solutions. Actual syringe concentrations are therefore twice that indicated above. [b] Values represent rate constants extracted from a single-exponential function. [c] AED-45 represents the V162C-AEDANS-45 protein.

Essentially, the same rate constant was observed when ATP-γ-S was substituted for ATP in the presence of the 44/62 complex (Table 3, row 3). The addition of DNA to the mixture containing ATP and the 44/62 complex did not appear to affect the observed 45 protein subunit exchange rate (Table 3, row 4). Under these conditions, the 45 protein will be rapidly cycling on and off DNA during subunit exchange (see Discussion). Formation of the holoenzyme complex on DNA (i.e., adding the T4 polymerase) reduced the observed 45 protein subunit exchange rate approximately 3-fold (Table 3, row 5).

DISCUSSION

In this paper, we have developed a fluorescence resonance energy transfer based assay to directly monitor intersubunit protein−protein interactions between subunits of the T4 DNA polymerase clamp (the 45 protein). Using either this assay or the variants of the 45 protein developed for this assay, it was possible to (a) obtain an estimate of the apparent trimeric 45 protein dissociation constant, (b) demonstrate that the 45 protein undergoes subunit exchange; and (c) show that while subunit exchange does not participate in the mechanism of 45 protein loading, it likely facilitates holoenzyme disassembly from DNA.

This subunit exchange study combines site-specific protein modification by fluorescent probes with the incorporation of unnatural amino acids. The introduction of unnatural amino acids into proteins has contributed to the analysis of protein structure/function relationships (for recent examples, see refs *29*, *30*, and *36*−*39*). Site-specific labeling of proteins with fluorescent probes has proved especially informative in numerous protein systems including T4 DNA replication (*24*, *25*).

In this paper a variant of the 45 protein was constructed that enables FRET between a tryptophan and a fluorescent probe across the subunit interface. This variant of the 45 protein contains an interfacial cysteine residue (V162C-45) alkylated with a fluorescent probe (IAEDANS) that can accept energy from excited tryptophan residues as shown in Figure 1. Upon dilution of the fluorescently labeled 45 protein (V162C-AEDANS protein), its specific fluorescence (λ_{ex} = 290 nm, λ_{em} = 488 nm) was diminished in a manner that could be fit to an equation derived from either a

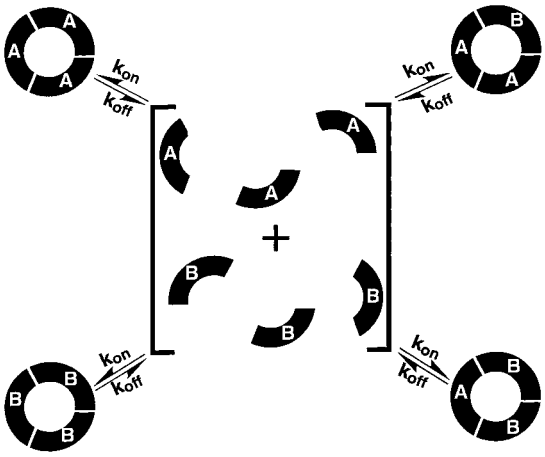

FIGURE 4: Model of 45 protein subunit exchange. Subunit exchange between the AEDANS-V162C-45 protein (A) and the nonfluorescent 4FW-45 protein (B) is illustrated as occurring via a cooperative dissociation (k_{off}) to monomers followed by a recombination (k_{on}) to form trimers. The FRET signal is observed across subunit interfaces of AEDANS-V162C-45 subunits (A). Upon exchange with subunits of the nonfluorescent 4FW-45 protein (B), the FRET signal is diminished. The equilibrium species distribution can be predicted by the binomial theorem (eq 8).

cooperative or a noncooperative model of trimerization (Figure 2, Table 2). The apparent K_d obtained from the cooperative model represents the product of the trimer to dimer dissociation constant (K_{d1}) and the dimer to monomer dissociation constant (K_{d2}). The equilibrium sedimentation analysis by Jarvis et al. (*27*) favors the cooperative model because they found the 45 protein to be trimeric at 5 μM, at which concentration the noncooperative model predicts that half (2.5 μM) of the protein is present as a dimer. Recently, the 45 protein trimeric dissociation constant was roughly estimated to be greater than 250 nM at 37 °C by a gel-filtration method (*20*). Although the difference in units prevents a direct comparison between the apparent K_d measured here (0.08 μM^2) and the estimate of Yao et al. (*20*), dissociation clearly occurs within the nanomolar range of protein concentrations indicated in Figure 2.

A nonfluorescent 45 protein was prepared by biosynthetically replacing native tryptophan residues with a 4-fluorotryptophan (4FW) analogue. The incorporation of 4FW into proteins has previously been shown to yield nonfluorescent proteins (*32*). The 4FW-45 protein served to demonstrate the occurrence of subunit exchange within the 45 protein by mixing it with the V162C-AEDANS protein. Subunit exchange between the above 45 proteins results in a loss of intersubunit FRET between the V162C-AEDANS and W91 on the opposing subunit. The observation of a decrease in the FRET signal upon subunit exchange serves to assign it as originating from energy transfer across the subunit interface (Figure 3).

Subunit exchange within the 45 protein can be described by the series of equilibria shown in Figure 4. Beginning with trimeric 45 protein, Figure 4 depicts subunit exchange as occurring via cooperative dissociation to form monomers that can recombine to form mixed trimers. It is evident that trimer dissociation is a first-order process whereas trimer association should exhibit higher order kinetic properties. Since subunit exchange was found to be representative of a

Table 4: Calculation of Observed Fluorescence Amplitude for 45 Protein Subunit Exchange at 25 °C

	cooperative					noncooperative				
	$F_{specific}$ (pM^{-1})	[initial] (nM)	$F_{initial}$	[equil^m] (nM)	F_{eq}	$F_{specific}$ (pM^{-1})	[initial] (nM)	$F_{initial}$	[equil^m] (nM)	F_{eq}
A	1.76	284	0.50	49.1	0.086	1.35	224	0.30	43	0.058
A_2	5.69[a]	0	0	0	0	6.32	294	1.86	11	0.070
AB	1.76[b]	0	0	0	0	1.35[b]	0	0	214	0.289
A_3	11.8	305	3.60	1.51	0.018	14.9	129	1.92	0.9	0.013
A_2B	5.69[a]	0	0	45.4	0.258	6.32[a]	0	0	26.7	0.169
AB_2	1.76[b]	0	0	454	0.799	1.35[b]	0	0	267	0.360
$\Sigma(F)$[c]	na	na	4.10/2 = 2.05[d]	na	1.16	na	na	4.08/2 = 2.04[d]	na	0.96

[a] The specific fluorescence of A_2B and A_2 was calculated from the sum of the intersubunit contribution at one interface (0.33 F_{A3}) and the intrasubunit contribution (F_A). [b] The specific fluorescence of AB_2 and AB was calculated from the residual intrasubunit contribution (F_A). [c] The initial protein concentrations were diluted 2-fold upon stopped-flow mixing. [d] The calculated amplitude for the cooperative model was 2.05−1.16 = 0.89, whereas for the noncooperative model it was 2.04−0.96 = 1.08.

first-order kinetic process in the observed range of protein concentrations, trimer dissociation must be rate-limiting (Figure 3).

Mixing the V162C-AEDANS protein with the 4FW-45 protein yields four species of varied subunit compositions (Figure 4). Assuming that the protein modifications do not bias the species population through specific subunit interactions, the equilibrium concentration of exchanged trimers can be simply predicted by the binomial theorem:

$$(x\mathrm{A} + y\mathrm{B})^3 = (x^3)\mathrm{A}_3 + (3x^2y)\mathrm{A}_2\mathrm{B} + (3xy^2)\mathrm{AB}_2 + (y^3)\mathrm{B}_3 \quad (7)$$

where A is the V162C-AEDANS monomer, B is the 4FW monomer, and x and y are their respective coefficients, in terms of protein concentrations. When 200 nM V162C-AEDANS trimer is mixed against 2000 nM 4FW-45 protein, the x coefficient becomes 200/2200 and y is 2000/2200. Substituting these values into eq 4 and multiplying through by the total 45 trimer concentration then produces

$$2200(0.091\mathrm{A} + 0.91\mathrm{B})^3 = 1.65\mathrm{A}_3 + 49.6\mathrm{A}_2\mathrm{B} + 496\mathrm{AB}_2 + 1653\mathrm{B}_3 \quad (8)$$

where the coefficients represent the equilibrium concentration (nanomolar) of the indicated species.

It is evident from Figure 4 that only the A_3 and A_2B species are capable of intersubunit FRET and from the above calculation that at equilibrium most of the V162C-AEDANS subunits are in a FRET-inactive mixed trimer (AB_2). The reduction in the amount of A_3, which contains three FRET-active subunit interfaces, and the formation of a small amount of A_2B, which contains only one FRET-active interface, should lead to an approximately 90% signal decrease. The finding that the FRET signal decayed maximally by about 45% in the presence of a 10-fold (Figure 3) or a 20-fold molar excess (data not shown) of the 4FW-45 protein can be attributed to the intrasubunit FRET contribution and the change in the relative population of species of trimers, dimers, and monomers from the initial to the final equilibrium state. The amplitudes for the kinetics of subunit exchange were calculated from either the cooperative or the noncooperative model by summing the fluorescent contribution from the anticipated distribution of V162C-AEDANS-containing species (Table 4). The total population of monomers, dimers, and trimers was determined from the appropiate expressions for trimer dissociation (eqs 1−3), and within a given species (e.g., dimers) the distribution of labeled and nonlabeled subunits was assigned from the coefficients of the binomial theorem (eq 7). The total fluorescence was then calculated from the sum of the products of the specific fluorescence (includes intrasubunit FRET contribution) and the relevant species concentration for the initial and final equilibrium condition with the amplitude being their difference (Table 4). Following these calculations, the FRET signals decayed by 43% (cooperative model) and 53% (noncooperative model). This exercise ties the data obtained from an equilibrium measurement of the dissociation process (Figure 2) to that observed for the kinetics of subunit exchange (Figure 3).

The subunit exchange kinetic data (Figure 3) was simulated by the KinSim program (*34*) using a sequence where the V162C-AEDANS trimer (A_3) dissociates through a dimer intermediate (A_2) to monomers (A), both of which can recombine with the nonfluorescent subunits (B or B_2) to diminish the observed intersubunit FRET signal (Scheme 1). The following assumptions were made in the simulation: (a) association rates between various labeled and unlabeled dimers and monomers were set equal ($k_1 = k_2 = k_3$), (b) dissociation rates for the various trimer species were corrected for statistical factors ($k_{-1}/3 = k_{-2}/2 = k_{-3}$), (c) the dissociation rates for dimeric species were presumed equal ($k_{-4} = k_{-5}$), and (d) the association rates for the dimer species were corrected for a statistical factor ($k_5 = 2k_4$). The K_d estimated from the dilution experiment (Figure 2) for either the cooperative (0.08 μM^2) or the noncooperative (0.51 μM, 0.17 μM) model was then used to reduce the number of independent variables in the simulation as $K_d = (k_{-1}k_{-4})/(k_1k_4)$, $K_{d1} = k_{-1}/k_1$, and $K_{d2} = k_{-4}/k_4$ (Scheme 1). The simulated concentrations of each species of the 45 protein were multiplied by their specific fluorescence and the products were summed for comparison to the observed exchange data (Figure 3; cooperative model shown). A similar good agreement was obtained from a simulation based on the noncooperative model (data not shown).

The main difference between the models is the origin of k_{obs}, which represents the trimer to dimer dissociation rate constant (0.01 s^{-1}) in the cooperative model, while the k_{obs} in noncooperative dissociation is influenced by both the trimer to dimer (0.019 s^{-1}) and dimer to monomer (0.0064 s^{-1}) rate constants. Estimates of the association rate constants were calculated using the K_d values for the

cooperative or the noncooperative model (Table 2) and the above apparent dissociation rate constants. The simulation also demonstrated that the observed rate constant was independent of both the total fluorescence change and the investigated range of 4FW-45 protein concentrations.

Having evaluated the kinetic scheme for subunit dissociation, one can now ask whether such steps are important in either loading the ring-shaped 45 protein onto DNA or its unloading from the holoenzyme•DNA complex. One potential mechanism for both loading and unloading the clamp is via a clamp oligomerization process. Previous estimates for the rate constant of holoenzyme formation are $1-2\ s^{-1}$ (*11*), which are at least 100-fold faster than the rates measured for subunit dissociation**.** The inability of the 44/62 complex to accelerate subunit dissociation therefore rules out subunit exchange on a kinetic basis as a mechanism of clamp loading (Table 3, rows 2 and 3). In fact, the slight inhibition observed in Table 3, rows 2 and 3 (relative to row 1), may be due to formation of a stoichiometric 45•44/62•ATP complex (*24*, *25*). Moreover, subunit exchange within the 45 protein was not altered during a cycle of continuous loading and dissociation from DNA, which on the basis of the steady-state ATPase rate (Table 1, 124 nM/s) dictates that all the 45 protein (2.2 μM) cycled through the DNA in less than 20 s (Table 3, row 4).

The time dependence for 45 protein subunit exchange is very similar to that reported for the dissociation of a stalled holoenzyme from DNA (*11*, *24*, *40*). Kaboord and Benkovic (*11*, *12*) reported that the holoenzyme dissociates from DNA according to a double-exponential function with approximate rate constants of 0.03 s^{-1} and 0.002 s^{-1} and relative amplitudes of 30% and 70%, which overlaps the rate constants for the loss of a single subunit at 0.003 s^{-1} (0.01 $s^{-1}/3$, cooperative model) and 0.07 s^{-1} (0.02 $s^{-1}/3$, noncooperative model). Consequently, an attractive hypothesis is that holoenzyme dissociation from DNA is mediated by 45 protein subunit dissociation. Formation of the holoenzyme reduced the observed rate of subunit exchange approximately 3-fold (Table 3, row 5), which suggests that only one subunit dissociates from the holoenzyme (Table 3, row 5). It is tempting to speculate that the stoichiometric holoenzyme complex prevents dissociation of two subunits by an interaction between the T4 polymerase C-terminus (*21*) and a subunit interface in the 45 protein. Further evidence that holoenzyme disassembly is mediated by clamp subunit dissociation follows from the finding that both the subunit exchange rate and the holoenzyme dissociation rate approximately doubled upon increasing the temperature from 25 to 37 °C (data not shown).

In conclusion, subunit exchange is not responsible for loading the 45 protein onto DNA during the process of holoenzyme formation. Subunit dissociation, however, appears to govern holoenzyme departure from DNA via loss of a 45 protein subunit. The fluorescence methods introduced here should continue to be useful in mechanistic investigations of the T4 DNA replication system.

ACKNOWLEDGMENT

We thank Ismail Moarefi and John Kuriyan for the structural coordinates of the 45 protein, Carl Frieden for supplying us with the W3110 *E. coli* strain, Theodore Carver, Steve Alley, Charles Scott, and Craig Cameron for thoughtful discussions, and Pat Benkovic for help in manuscript preparation.

REFERENCES

1. Alberts, B. M. (1987) *Philos. Trans. R. Soc. London, Ser. B 317*, 395−420.
2. Cha, T. A., and Alberts, B. M. (1988) *Cancer Cells 6*, 1−10.
3. Nossal, N. G. (1994) in *Molecular Biology of Bacteriophage T4* (Karam, J. D., Ed.) pp 43−55, American Society for Microbiology, Washington, DC.
4. Sexton, D. J., Berdis, A. J., and Benkovic, S. J. (1997) *Curr. Opin. Chem. Biol. 1*, 316−322.
5. Kuriyan, J., and O'Donnell, M. (1993) *J. Mol. Biol. 234*, 915−925.
6. Kelman, Z., and O'Donnell, M. (1995) *Annu. Rev. Biochem. 64*, 171−200.
7. Kong, X. P., Onrust, R., O'Donnell, M., and Kuriyan, J. (1992) *Cell 69*, 425−437.
8. Krishna, T. S. R., Kong, X. P., Burgers, P. M., and Kuriyan, J. (1994) *Cell 79*, 1233−1243.
9. Nossal, N. G. (1992) *FASEB J. 6*, 871−878.
10. Young, M. C., Reddy, M. K., and von Hippel, P. H. (1992) *Biochemistry 31*, 8675−8690.
11. Kaboord, B. F., and Benkovic, S. J. (1995) *Curr. Biol. 5*, 149−157.
12. Kaboord, B. F., and Benkovic, S. J. (1996) *Biochemistry 35*, 1084−1092.
13. Tinker, R. L., Williams, K. P., Kassavetis, G. A., and Geiduschek, E. P. (1994) *Cell 77*, 225−237.
14. Tinker, R. L., Kassavetis, G. A., and Geiduschek, E. P. (1994) *EMBO J. 13*, 5330−5337.
15. Gogol, E. P., Young, M. C., Kubasek, W. L., Jarvis, T. C., and von Hippel, P. H. (1992) *J. Mol. Biol. 224*, 395−412.
16. Fu, T.-J., Sanders, G. M., O'Donnell, M., and Geiduschek, E. P. (1996) *EMBO J. 15*, 4414−4422.
17. Herendeen, D. R., Kassavetis, G. A., Barry, J., Alberts, B. M., and Geiduschek, E. P. (1989) *Science 245*, 952−958.
18. Herendeen, D. R., Williams, K. P., Kassavetis, G. A., and Geiduschek, E. P. (1990) *Science 248*, 573−578.
19. Herendeen, D. R., Kassavetis, G. A., and Geiduschek, E. P. (1992) *Science 256*, 1298−1303.
20. Yao, N., Turner, J., Kelman, Z., Stukenberg, P. T., Pan, Z.-Q., Hurwitz, J., and O'Donnell, M. (1996) *Genes Cells 1*, 101−113.
21. Berdis, A. J., Soumillion, P., and Benkovic, S. J. (1996) *Proc. Natl. Acad. Sci. U.S.A. 93*, 12822−12827.
22. Goodrich, L. D., Lin, T. C., Spicer, E. K., Jones, C., and Konigsberg, W. H. (1997) *Biochemistry 36*, 10474−10481.
23. Berdis, A. J., and Benkovic, S. J. (1996) *Biochemistry 35*, 9253−9265.
24. Sexton, D. J., Carver, T. E., Berdis, A. J., and Benkovic, S. J. (1996) *J. Biol. Chem. 271*, 28045−28051.
25. Latham, G. J., Pietroni, P., Dong, F., Young, M. C., and von Hippel, P. H. (1996) *J. Mol. Biol. 264*, 426−439.
26. Frey, M. W., Nossal, N. G., Capson, T. L., and Benkovic, S. J. (1993) *Proc. Natl. Acad. Sci. U.S.A. 90*, 2579−2583.
27. Jarvis, T. C., Paul, L. S., and von Hippel, P. H (1989) *J. Biol. Chem. 264*, 12709−12716.
28. Morris, C. F., Hama-Inaba, H., Mace, D., Sinha, N. K., and Alberts, B. M. (1979) *J. Biol. Chem. 254*, 6787−6796.
29. Soumillion, P., Jespers, L., Vervoort, J., and Fastrez, J. (1995) *Protein Eng. 8*, 451−456.
30. Hoeltzli, S. D., and Frieden, C. (1994) *Biochemistry 33*, 5502−5509.
31. Sambrook, J., Fritsch, E. F., and Maniatis, T. (1989) in *Molecular Cloning: A Laboratory Manual*, Cold Spring Harbor Laboratory Press, Cold Spring Harbor, NY.
32. Bronskill, P. M., and Wong, T.-F. (1988) *Biochem. J. 249*, 305−308.
33. Weast, R. C., and Selby, S. M. (1970) in *Handbook of Tables for Mathematics* (Weast, R. C., and Selby, S. M., Eds.) pp 129−131, CRC Press, Cleveland, OH.

34. Frieden, C. (1994) *Methods Enzymol. 240,* 311−322.
35. Lakowicz, J. R. (1983) in *Principles of Fluorescence Spectroscopy*, Plenum Press, New York.
36. Laue, T. M., Senear, D. F., Eaton, S., and Ross, J. B. A. (1993) *Biochemistry 32,* 2469−2472.
37. Koide, H., Yokoyama, S., Katayama, Y., Muto, Y., Kigawa, T., Kohno, T., Takusari, H., Oishi, M., Takahashi, S., Tsukumo, K., et al. (1994) *Biochemistry 33,* 7470−7476.
38. Budisa, N., Steipe, B., Damange, P., Eckerskorn, C., Kellermann, J., and Huber, R. (1995) *Eur. J. Biochem. 230,* 788−796.
39. Beiboer, S. H. W., van den Berg, B., Dekker: N., Cox, R. C., and Verheij, H. M. (1996) *Protein Eng. 9,* 345−352.
40. Hacker, K. J., and Alberts, B. M. (1994) *J. Biol. Chem. 269,* 24209−24220.

BI972526A